On the Impact of Discrete Secondary Controllers on Power System Dynamics

Taulant Kërçi, *Student Member, IEEE*, Mohammed Ahsan Adib Murad, Ioannis Dassios, and Federico Milano, *Fellow, IEEE*

***Abstract*—This paper discusses the impact of discrete secondary controllers on the dynamic response of power systems. The idea of the paper originates from the observation that there is a range of values, from few tens of seconds to few minutes, of the execution cycles of conventional automatic generation control (AGC) that leads to a limit cycle. Below and above this range the system is stable. This is certainly not a problem in practice as the AGC updates the power set points of generating units every few seconds. However, this phenomenon has interesting consequences if one considers real-time electricity markets with short dispatch periods (i.e., 5 minutes) as these markets can be modeled as a sort of AGC. The paper first provides a formal analogy between conventional AGC and real-time electricity markets. Then it shows that the discretization-driven instability exists if the system includes a real-time electricity market modeled as secondary frequency controller. Finally, the paper discusses the impact of the combined effect of high wind generation shares and discrete secondary controllers on power system dynamics.**

***Index Terms*—Automatic generation control, power system stability, real-time electricity market, discretization.**

I. Introduction

A. Motivation

THE automatic generation control (AGC) is a centralized secondary regulator implemented in the control centers of Transmission System Operators (TSOs). Its main function is to adjust the generation of the dispatchable generating units, e.g. thermal and hydro, to keep frequency deviations and tie-line interchanges of each TSO control area within specified values [1]. Consequently, the effectiveness of this control depends on the characteristics of the controlled generating units. Typically, AGC dynamics take place in the time scale of minutes, e.g. 10 minutes [2]. In practice, the AGC is implemented in a discrete form. That is, the AGC sends power signals to participating generating units at fixed intervals, e.g. every 2-6 seconds [3], [4]. This time interval has shown to be adequate in managing real-time power mismatches and, to the best of our knowledge, has not caused any power system instability. In view of the discussion carried out in this paper, however, it is relevant to investigate the effect of increasing this time interval.

The first part of this paper thoroughly discusses this scenario and shows that there is a range of values, from few tens of seconds to few minutes, of the execution cycles of conventional AGC that leads to a limit cycle. This result serves as a motivation to study the same phenomenon when considering real-time electricity markets with short trading intervals. In fact, these markets are currently moving to 5 minutes or even faster trading intervals in order to facilitate the integration of high shares of renewable energy sources (RES) into power systems. The Australian energy market operator, for example, manages a real-time electricity market with 5 minutes dispatch intervals and is planning to align the dispatch and financial settlement periods by July 2021 [5]. These time scales are comparable with those of the AGC. Motivated by this fact and by the observation that real-time market can be modeled as a sort of discrete AGC, we make use of a dynamic electricity market model proposed in [6] and discretize it to represent different trading intervals. Then, we investigate the impact of the Market-based Automatic Generation Control (MAGC) on the power system stability when using different trading intervals and different shares of renewable generation.

B. Literature Review

The concept of "sample-data system" has been widely discussed in the literature, and so has the effect of the sampling period on stability. For example, reference [7] proposes a linear matrix inequality (LMI)-based delay-dependent stability criterion that allows calculating the delay margins of multi-area load frequency control (LFC) schemes and choosing the upper bound of the sampling period. More recently, [8] presents a study on the stability of time-delayed cyber-physical power systems under fully distributed frequency control using a critical eigenvalue tracking algorithm. However, references [7] and [8] consider only time delays, not discrete controllers. Delay-dependent controllers are, in effect, quite different compared to the discrete controllers considered in this work. That is, the former act continuously but use quantities that are "old," while the latter act "now" on the current value of the measured signal and then do nothing during a given period.

Manuscript received July 20, 2020; revised January 27, 2021 and February 16, 2021; accepted February 20, 2021. Date of publication February 23, 2021; date of current version August 19, 2021. This work was supported by Science Foundation Ireland, by funding T. Kërçi and F. Milano under project ESIPP, Grant No. SFI/15/SPP/E3125, and M. A. A. Murad, I. Dassios and F. Milano under project AMPSAS, Grant No. SFI/15/IA/3074. Paper no. TPWRS-01212-2020. *(Corresponding author: Federico Milano.)*

The authors are with the School of Electrical & Electronic Engineering, University College Dublin, Dublin 4, Dublin, Ireland (e-mail: taulant.kerci@ucdconnect.ie; mohammed.murad@ucdconnect.ie; ioannis.dassios@ucd.ie; federico.milano@ucd.ie).

Digital Object Identifier 10.1109/TPWRS.2021.3061584

Reference [9] proposes a robust proportional-integral LFC scheme that takes into account the sampling period and the transmission delay of the communication network. Reference [10] designs a robust retarded sampled-data control with constant delays and proposes a delay-dependent sufficient criterion in the form of LMIs in order to improve the dynamic performance of power systems with the inclusion of RES. While [9] and [10] consider sampling periods along with communication delays, these references do not discuss the phenomenon of the limit cycles that arise for large sampling periods. A detailed discussion on the birth of these limit cycles is included in this paper. Moreover, [9] and [10] consider time periods up to a maximum of 14 seconds, which, as shown in this paper, are hardly an issue for secondary controllers.

It is also relevant to note that all four references above, namely, [7]–[10], utilize a linear state-space representation of the system and, in general, very simplified models (e.g., 2nd order classical model of synchronous machines). On the other hand, the analysis that carried out in the remainder of this paper is based on a set of fully-fledged nonlinear differential-algebraic equations for transient stability analysis. This is a crucial difference of our approach with respect to existing literature.

Other relevant examples are [11] and [12] that focus on short-term dynamics of linear systems. Existing literature, thus, has not yet thoroughly discussed the impact of discrete controllers on the long-term dynamics of nonlinear hybrid systems. On the other hand, research works that have utilized the market model in [6] to study its impact on power system dynamics, are based on small-signal stability analysis, e.g. [13]. In [14], the authors utilize the market model in [6] to study the impact of grid-connected microgrids, but do not provide a formal analogy between AGC and MAGC. Finally, among the works that have used the model proposed in [6] to study the stability of electricity markets, we cite, for example, [15] and [16].

C. Contributions

The main contributions of this paper are as follows:

- Provide a systematic study on the impact of discrete secondary controllers on power system dynamics.
- Present a formal analogy between AGC and MAGC.
- Show that the time periods of discrete AGC and MAGC may give raise to limit cycles.
- Investigate the impact of discrete AGC on systems with high shares of wind power generation.

D. Paper Organization

The rest of the paper is organized as follows. Section II describes the hybrid model of power systems used for dynamic studies. Section III discusses the model of the AGC as well as the impact of its time interval. Section IV presents a formal analogy between AGC and MAGC, and provides a thorough analysis on the impact of the time period on both controllers. Section V focuses on the impact of wind power penetration on the performance of both AGC controllers as well as power system dynamic response. Finally, Section VI draws conclusions and outlines future work directions.

II. Hybrid Power System Model

Power systems can be modeled as a set of nonlinear Hybrid Differential-Algebraic Equations (HDAEs) [17], as follows:

$$\begin{aligned} \dot{\boldsymbol{x}} &= \boldsymbol{f}(\boldsymbol{x}, \boldsymbol{y}, \boldsymbol{u}, \boldsymbol{z}) \,, \\ \mathbf{0}_{n_y,1} &= \boldsymbol{g}(\boldsymbol{x}, \boldsymbol{y}, \boldsymbol{u}, \boldsymbol{z}) \,, \end{aligned} \tag{1}$$

where $\boldsymbol{f}$ are the differential equations, $\boldsymbol{g}$ are the algebraic equations, $\boldsymbol{x}$, $\boldsymbol{x} \in \mathbb{R}^{n_x}$ are the state variables, e.g. generator rotor speeds, and $\boldsymbol{y}$, $\boldsymbol{y} \in \mathbb{R}^{n_y}$, are the algebraic variables, e.g. bus voltage angles; $\boldsymbol{u}$, $\boldsymbol{u} \in \mathbb{R}^{n_u}$, are the inputs, e.g. load forecast, generator bids; and $\boldsymbol{z}$, $\boldsymbol{z} \in \mathbb{N}^{n_z}$, are the discrete variables, e.g. status of the machines. The functions $\boldsymbol{f}, \boldsymbol{g}$ are at least C^1.

The set of nonlinear HDAEs (1) is a special case of a singular system of nonlinear hybrid differential equations in the following form:

$$\mathbf{E}\dot{\boldsymbol{\xi}} = \boldsymbol{F}(\boldsymbol{\xi}, \boldsymbol{u}, \boldsymbol{z}) \,, \tag{2}$$

where

$$\mathbf{E} = \begin{bmatrix} \mathbf{I}_{n_x} & \mathbf{0}_{n_x,n_y} \\ \mathbf{0}_{n_y,n_x} & \mathbf{0}_{n_y,n_y} \end{bmatrix}, \quad \boldsymbol{\xi} = \begin{bmatrix} \boldsymbol{x}(t) \\ \boldsymbol{y}(t) \end{bmatrix},$$

and

$$\boldsymbol{F}(\boldsymbol{\xi}, \boldsymbol{u}, \boldsymbol{z}) = \begin{bmatrix} \boldsymbol{f}(\boldsymbol{x}, \boldsymbol{y}, \boldsymbol{u}, \boldsymbol{z}) \\ \boldsymbol{g}(\boldsymbol{x}, \boldsymbol{y}, \boldsymbol{u}, \boldsymbol{z}) \end{bmatrix}.$$

An hybrid system is a set of systems of differential equations where transition conditions from one system to another in that set of systems play an important role. This can be easily seen from the following example. Let $\boldsymbol{z} \in \{\boldsymbol{z}_1, \boldsymbol{z}_2\}$, $\boldsymbol{z}_1, \boldsymbol{z}_2$ constant vectors in $\mathbb{N}^{n_z}$; $\boldsymbol{z}_1, \boldsymbol{z}_2$ can then be considered as two different modes and (2) can be split into two systems:

$$\mathbf{E}\dot{\boldsymbol{\xi}} = \boldsymbol{F}(\boldsymbol{\xi}, \boldsymbol{u}, \boldsymbol{z}_1), \qquad \mathbf{E}\dot{\boldsymbol{\xi}} = \boldsymbol{F}(\boldsymbol{\xi}, \boldsymbol{u}, \boldsymbol{z}_2) \,.$$

In this case, there will be two systems of singular non-linear differential equations. However, the index set of the mode transitions as well as the transition conditions should be taken into account and defined. In general, (2) can be rewritten as $\mathbf{E}\dot{\boldsymbol{\xi}} = \boldsymbol{F}(\boldsymbol{\xi}, \boldsymbol{u}, \boldsymbol{z}_i)$, $i = 0, 1, 2, \ldots, N$, $\boldsymbol{z}_i$ constant. Then each singular nonlinear system is only defined in a certain interval $t \in [t_i, t_{i+1})$, $i = 0, 1, 2, \ldots, N$.

Equations (1) and (2) are utilized to emulate the transient behavior of power systems. These equations include the dynamic models of synchronous machines, turbine governors (TGs), automatic voltage regulators, power system stabilizers and the discrete model of the AGC and MAGC. In addition to the AGC and MAGC, a brief description of the model of the TGs is given below. The interested reader is referred to [17] for a detailed description of all others models.

It is important to note that tools for the stability analysis of nonlinear hybrid dynamical systems are quite limited. The nonlinearity prevents the use of methods that require a linear set of equations and this eliminates the vast majority of available techniques. The Lyapunov stability theory has been widely utilized for the analysis of nonlinear systems, including power systems. However, due to the dissipative nature of power systems, even assuming that a Lyapunov function can be found,

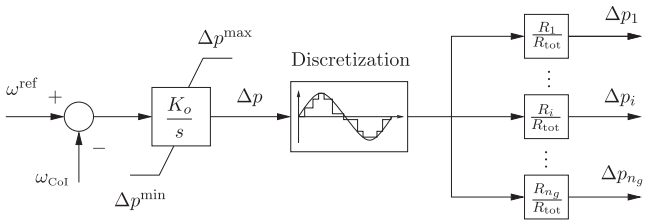

Fig. 1. AGC control diagram.

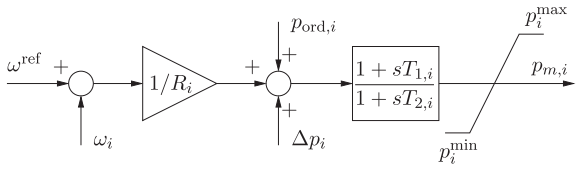

Fig. 2. Turbine governor control diagram.

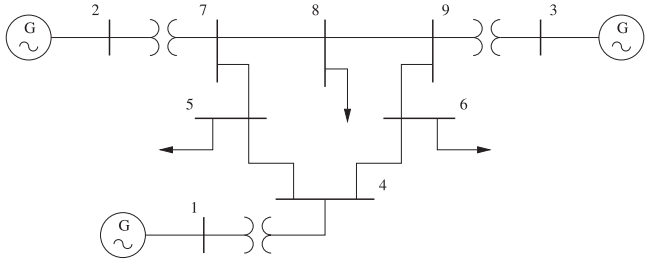

Fig. 3. Single line diagram of the IEEE WSCC 9-bus system.

the Lyapunov theory would not provide sufficient and necessary conditions and is thus of limited practical use. The only fully general approach to study the stability of power systems that does not requires shortcuts or simplifications is the time-domain simulation. This is the approach utilized in this work.

III. Conventional AGC

The main function of the AGC controller is to maintain the balance between the total electricity supply and demand. This action is achieved through continuously monitoring the MW output of the controllable generating units. Fig. 1 shows a standard control scheme of an AGC. The input of the controller is the difference between the reference frequency ω^{ref} and the measured frequency ω_{CoI}, that is, the Center of Inertia (CoI). Note that in practice TSOs use the frequency of a pilot bus of the system as an input for the AGC. Next, the main controller of the AGC is an integral control with gain K_o, as follows:

$$\Delta\dot{p} = K_o(\omega^{\text{ref}} - \omega_{\text{CoI}})\,, \tag{3}$$

where Δp is the output of the integrator. The integral term is needed to perfect tracking the reference frequency and nullify the steady-state frequency error introduced by the primary control. In general, TSOs use AGC based on proportional integral controller that includes other functionalities, among others, filtering and heuristics in order to reduce the area control error [18]. However, the fact that ω_{CoI} is used as an input for the controller represents actually a sort of filter (i.e., it filters local frequency oscillations due to its weighted nature). The output of the continuous integrator is discretized at given fixed-time intervals and sent to each TG.

These signals (Δp_i) are proportional to the capacity of the machines and the TG droops (R_i) and normalized with respect to the total droop of the system:

$$R_{\text{tot}} = \sum_{i=1}^{n_g} R_i\,. \tag{4}$$

The model of the TG considered in this work is depicted in Fig. 2. It is composed of a droop R_i and a lead lag transfer function. $T_{1,i}$ and $T_{2,i}$ represent the transient gain and governor time constant, respectively. $p_{\text{ord},i}$ represent the power order set-point as obtained by the electricity market (see section IV). This model is suitable for transient stability analysis [17].

In practice, the output of the AGC is limited by the secondary regulation reserve [4]. Therefore, the active power output of the integrator block of the AGC (see Δp in Fig. 1) is limited [19], in this case, through an anti-windup (AW) limiter, as follows:

$$\begin{aligned}
&\text{if } \Delta p \geq \Delta p^{\max} \;\&\; \Delta\dot{p} \geq 0 : \Delta p = \Delta p^{\max} \;\&\; \Delta\dot{p} = 0\,,\\
&\text{if } \Delta p \leq \Delta p^{\min} \;\&\; \Delta\dot{p} \leq 0 : \Delta p = \Delta p^{\min} \;\&\; \Delta\dot{p} = 0\,,\\
&\qquad\qquad \text{otherwise}: \;\Delta\dot{p} = K_o(\omega^{\text{ref}} - \omega_{\text{CoI}})\,.
\end{aligned} \tag{5}$$

The AW limiter is needed to limit the windup phenomenon of the integrator state variable (Δp).

A. Illustrative Example on the AGC

In this section we present an illustrative example on the impact of discrete AGC on power system stability. The IEEE WSCC 9-bus system (see Fig. 3) is used to show the effect of different AGC time intervals. The base case data of this network can be found in [20].

Since the original benchmark system does not include an AGC, we have included in the model the AGC described in the previous section. In the simulation results below, the disturbance consists in the disconnection of the load at bus 6 at $t = 1$ s. All simulations in this paper are performed using the power system analysis software tool Dome [21].

1) Sensitivity Analysis With Respect to K_o: We first consider the effect of K_o with a continuous AGC model. It is well-known that a high gain of the AGC may lead to power system instability due to the coupling between the dynamics of the primary frequency control and AGC. Fig. 4 shows the transient behavior of ω_{CoI} for $K_o = \{5, 20, 50\}$ without considering the AW limiter; and for $K_o = 100$ with inclusion of the AW limiter on Δp (40% of the total generation capacity). As expected, the system is unstable for high values of K_o, in this case, for $K_o > 20$. On the other hand, low gain values keep the system stable (see Fig. 5). However, the dynamic response with this small value of K_o is very slow, and consequently the controller is not effective. Finally, imposing a limiter on Δp leads to a limit cycle.

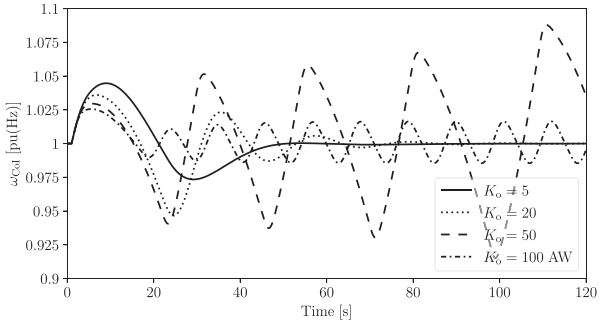

Fig. 4. Transient response of ω_{CoI} of the WSCC 9-bus system for different AGC gains.

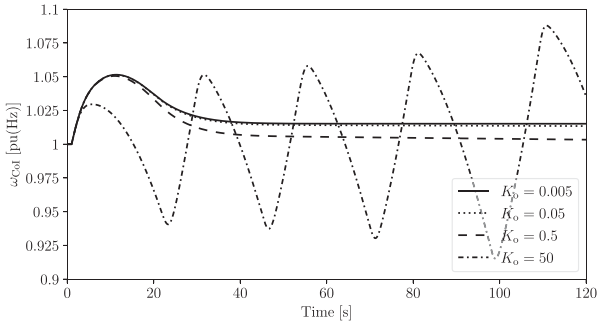

Fig. 5. Transient response of ω_{CoI} of the WSCC 9-bus system for different AGC gains.

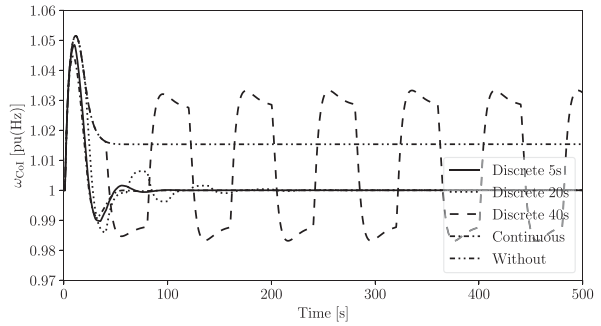

Fig. 6. Transient response of ω_{CoI} for different AGC time intervals.

2) Impact of Different AGC Time Intervals: First we show qualitatively that the impact of different values of K_o of continuous AGC is equivalent to different time intervals of a discrete AGC. Let us discretize the first-order differential equation (3) using the forward Euler method. The k-th integration step is:

$$\Delta p^{(k+1)} = K_o \Delta t(\omega^{\mathrm{ref}} - \omega_{\mathrm{CoI}}) + \Delta p^{(k)}\,, \tag{6}$$

where $\Delta p^{(k+1)}$ and $\Delta p^{(k)}$ are the next and present value of Δp, respectively; Δt is the integration time interval. From (6), it is apparent that increasing Δt is equivalent to increasing K_o.

Figs. 6 and 7 depict the transient response of the ω_{CoI} for different AGC time intervals. Observe that using a continuous AGC and a discrete AGC with a time interval of 5 and 20 s, the system is stable as the controller is fast enough to bring back the

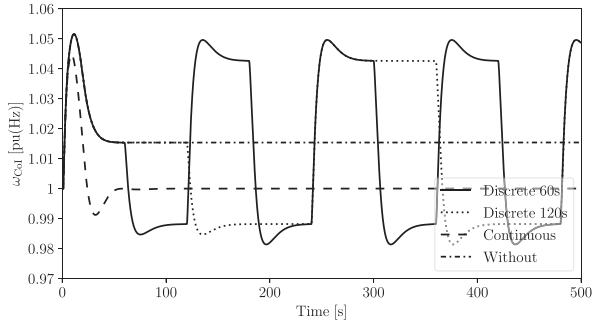

Fig. 7. Transient response of ω_{CoI} for different AGC time intervals.

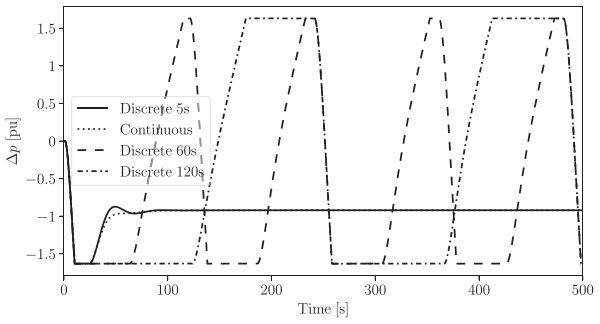

Fig. 8. Transient response of Δp for different AGC time intervals.

frequency to the nominal value. On the other hand, the results without an AGC show a stable transient response with a steady state-frequency error. For AGC time intervals equal or greater than 40 s, the system enters into a limit cycle. As expected from the discussion above, large discretization time intervals lead to unstable system dynamics. For this reason, in practice, the AGC time interval is in the range of $(2, 6)$ s, which is small enough not to originate any limit cycle.

Fig. 8 shows the transient behavior of the state variable of the AGC (Δp) for some relevant AGC time intervals. The limit cycle occurs whenever the AGC time interval is big enough (e.g. 120 s) to allow Δp to go to the other extreme value (limit) and saturate. Other factors that determine the period of the limit cycle are related to how fast is the AGC controller as well as the type of the contingency. Note that for very long-time intervals, e.g. > 10 minutes, the AGC controller is not effective anymore and other mechanisms are in place to compensate the power unbalance e.g. short-term optimal power flow.

3) RoCoF Dead-Band: A way to remove the bang-bang phenomena shown in the previous section is to consider a dead-band on the Rate of Change of Frequency (RoCoF). In this work, the RoCoF is calculated using the following expression:

$$\mathrm{RoCoF} = \frac{\omega_{\mathrm{CoI}}^{(k-1)} - \omega_{\mathrm{CoI}}^{(k)}}{\Delta t}\,, \tag{7}$$

where $\omega_{\mathrm{CoI}}^{(k-1)}$ and $\omega_{\mathrm{CoI}}^{(k)}$ correspond to the values of ω_{CoI} at the previous interval (e.g., 5 seconds) and the current time, respectively. While Δt represents the AGC time interval. Note that controlling the frequency of the CoI is not viable in practice.

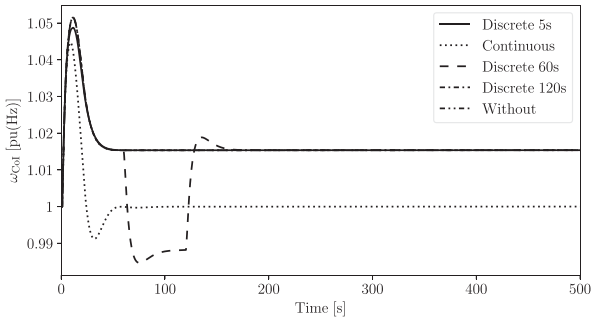

Fig. 9. Transient response of ω_{CoI} for different AGC time intervals and with RoCoF dead-band.

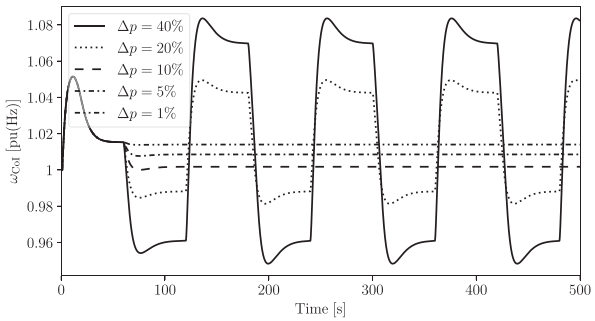

Fig. 10. Transient response of ω_{CoI} for different Δp limits.

One can, however, implement RoCoF dead-bands in the primary frequency controllers of the power plants. These will affect the variation of the rotor speeds of the synchronous machines and, in turn, of the frequency of the CoI. The model considered in the paper is thus an approximation but it is sufficient to show the effect of this dead-band.

Fig. 9 depicts the transient behavior of the ω_{CoI} with RoCoF dead-band of 0.0002 pu(Hz/s). The RoCoF dead-band successfully removes the limit cycle, however, it leads to a frequency steady-state error. Clearly, this is not desirable because the AGC cannot serve its main purpose.

4) Sensitivity Analysis With Respect to Δp: Another solution to prevent the bang-bang phenomena is to limit the variation of the internal state variable of the AGC, namely, Δp. The limit case, of course, is when the limit of $\Delta p^{\max} = \Delta p^{\min} = 0$, which basically opens the control loop. Fig. 10 depicts the transient behavior of the ω_{CoI} for a variation of Δp from 40% up to 1% and for an AGC time interval of 60 seconds. As expected, limiting Δp makes the AGC controller less effective. For example, allowing Δp to vary just 1% of the total generation capacity, is almost equivalent to disabling the AGC.

Based on the simulation results above, we conclude that the only effective solution to avoid the limit cycle phenomena caused by the discretization of the AGC is to impose a sufficiently small Δt.

IV. Market-Based AGC

In this section, we provide a formal analogy between secondary controllers and the dynamic electricity market proposed by Alvarado in [6]. Moreover, this section discusses the impact of this discrete controller on the dynamic response of the system.

A. Dynamic Electricity Market Model

Alvarado started to study the dynamics of electricity markets after similar works were performed by economists in their respective fields [22]. The main idea behind his studies on this topic was to be able to manage the real-time balance between power demand and supply through a continuous price signal sent to both loads and generators.

In this model, it is assumed that when a generator sees that the electricity price, say, λ, is higher/lower than the corresponding marginal cost, then the generator will increase/decrease its production until the cost matches the price. These assumptions lead to the following dynamic electricity market model [6]:

$$T_\lambda \dot{\lambda} = K_E(\omega^{\mathrm{ref}} - \omega_{\mathrm{CoI}}) - D_\lambda \lambda\,, \tag{8}$$

$$T_{g,i}\Delta\dot{p}_{g,i} = \lambda - c_{g,i}\Delta p_{g,i} - b_{g,i}\,, \quad i = 1, \ldots, n_g\,, \tag{9}$$

where $\Delta p_{g,i}$ represent the active power order set points ($p_{\mathrm{ord},i}$) of the TGs (see Fig. 2); $c_{g,i}$ and $b_{g,i}$ are the parameters of the marginal benefit of the generators. T_λ and $T_{g,i}$ are the time constants; and K_E is the feedback gain. D_λ is the deviation with respect to a perfect tracking integrator and for a low-pass filter is $D_\lambda = 1$. Finally, the mismatch $\omega^{\mathrm{ref}} - \omega_{\mathrm{CoI}}$ is utilized as an indirect estimation of the real-time energy imbalance in the system.

In [6], loads responds similarly to generators with respect to the electricity price λ but with opposite strategy, i.e. load bids increase as the electricity price decreases. In this paper, however, loads are assumed to be inelastic and do not participate in the MAGC. Such an assumption is consistent with the current situation in most of the electricity markets where loads (effectively) do not respond to changes in the wholesale electricity prices. In fact, it has been shown in the literature that making loads price responsive as well will further deteriorate the stability of the system [15].

Note that the use of this electricity market model (8)-(9) is considered adequate for real-time markets with short dispatch periods [6]. As mentioned earlier in the paper, some systems already use these markets and they will be more common in the future power systems.

B. Analogy Between AGC and MAGC

The structure of the equations (8)-(9) is formally similar to the structure of the AGC shown in Fig. 1. For comparison, the "control" diagram of (8)-(9) is depicted in Fig. 11. The AGC and the MAGC have exactly the same structure for $D_\lambda = b_{g,i} = T_{g,i} = 0$. The MAGC can be thus seen as a generalized secondary frequency controller.

A substantial difference between the two controllers concerns the meaning of the state variables, namely Δp and λ. In the MAGC, λ is a price, which does not carry any information on the energy involved in the system, as opposed to Δp, which is a power reserve. Nevertheless, the market model (8)-(9) makes λ a "physical quantity" of the system.

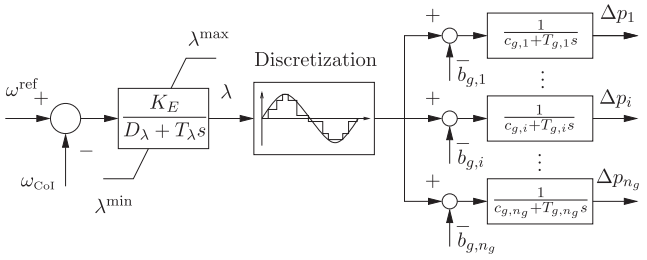

Fig. 11. MAGC control diagram.

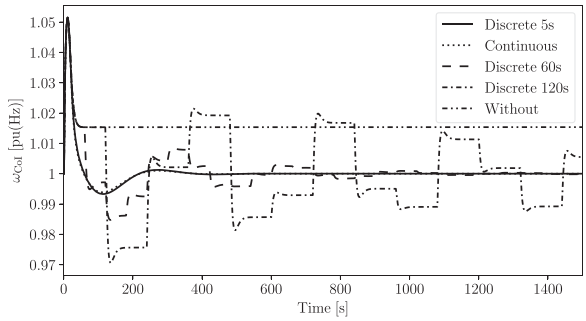

Fig. 12. Transient response of ω_{CoI} for different MAGC time intervals.

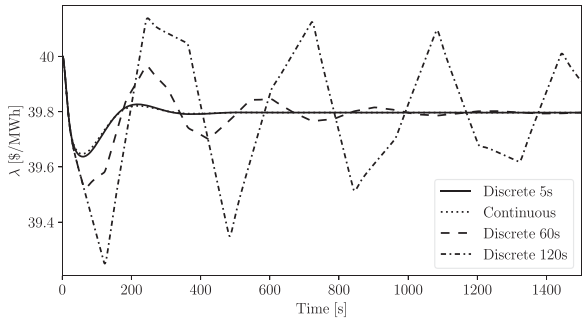

Fig. 13. Transient response of the electricity price λ for different MAGC time intervals.

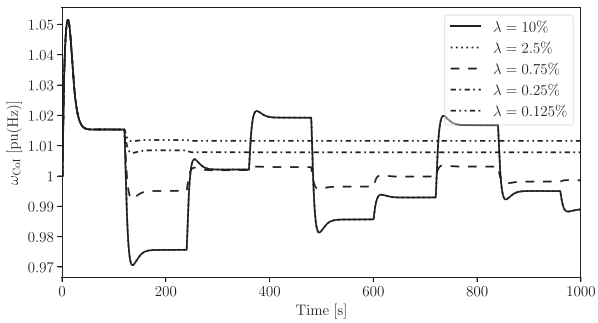

Fig. 14. Transient response of ω_{CoI} for different λ limits.

C. Anti-Windup Limiter on λ

Similar to the AW limiter on Δp, one can limit the state variable of the MAGC, namely, λ in Fig. 11. Enforcing a limit on λ might be desirable in order to limit the electricity price spikes. This happens, for example, in most of the European electricity markets [23]. The AW limiter on λ is as follows:

$$\begin{aligned} &\text{if } \lambda \geq \lambda^{\max} \;\&\; \dot{\lambda} \geq 0 : \lambda = \lambda^{\max} \;\&\; \dot{\lambda} = 0, \\ &\text{if } \lambda \leq \lambda^{\min} \;\&\; \dot{\lambda} \leq 0 : \lambda = \lambda^{\min} \;\&\; \dot{\lambda} = 0, \\ &\text{otherwise : equation (8)}. \end{aligned} \tag{10}$$

D. Illustrative Example on the MAGC

The analogy discussed in Section IV-B allows us simulating real-time electricity markets as an equivalent AGC. In this case, however, the time interval matters because in practice electricity markets use dispatch periods of the order of minutes, not seconds as in the conventional AGC.

For a fair comparison between the AGC and MAGC, we use again the IEEE WSCC 9-bus system and we assume that the three generators have the same market data as the first three generators in the IEEE 39-bus system [6]. Unless stated otherwise, for simulation purposes, the maximum and minimum limit of λ is set to 4000 and 0 $/MWh, respectively. The contingency is the outage of the load at bus 6 at $t = 1$ s.

1) Systems With MAGC Only: In this first scenario, it is assumed that the system includes only the MAGC controller, i.e. there is no AGC. This scenario corresponds to power systems that do not include an AGC, but instead use some sort of offline and/or "manual" generation control [18]. The goal is to investigate whether the idea of controlling power systems exclusively based on market mechanism is feasible.

Figs. 12 and 13 show the transient behavior of ω_{CoI} and λ, respectively. The discrete MAGC leads to limit cycles similar to the case of the AGC. Specifically, the limit cycle appears for a MAGC time interval equal or above 120 s. Compared to the AGC, this phenomenon appears for longer time intervals, i.e. double in this case. This is due to the parameters of the MAGC control scheme. It is important to note, however, that the limit cycles always appear for a certain range of Δt, independently from the parameters of the secondary controller.

There are two ways to avoid the limit cycles. One is to use "short" time periods, for example, 5 s in Fig. 12. The other one is to use "long" time periods, for example, 10 minutes [24]. In this case, the MAGC approximation does not hold and is effectively decoupled from the dynamics of the system, and thus it does not cause the occurrence of instability. Fig. 12 also suggests that real-time electricity markets with very short periods, e.g. 5 s, can, in principle, substitute the AGC provided that they have the same features.

2) Sensitivity Analysis With Respect to λ: As discussed earlier in the paper, a solution to remove the limit cycle is to limit the variation of the state variable of the AGC controller, in this case, that of MAGC controller. In this context, Fig. 14 shows the transient response of the system for different λ limits. As expected, limiting the variation of the state variable removes the limit cycle. For example, allowing λ to vary just 0.25% from its nominal value (40 $/MWh) appears to be able to remove the instability, however, it leads to a steady state frequency error. Further limiting the variation of λ, e.g. 0.125%, makes

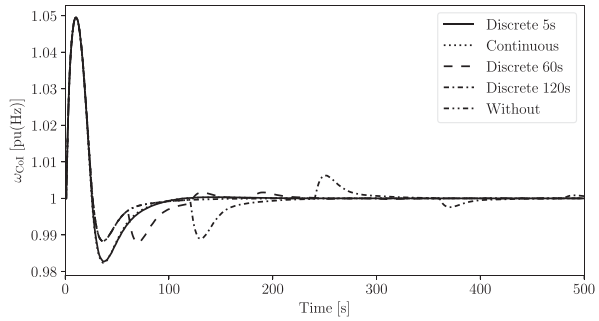

Fig. 15. Transient response of ω_{CoI} using the AGC and MAGC.

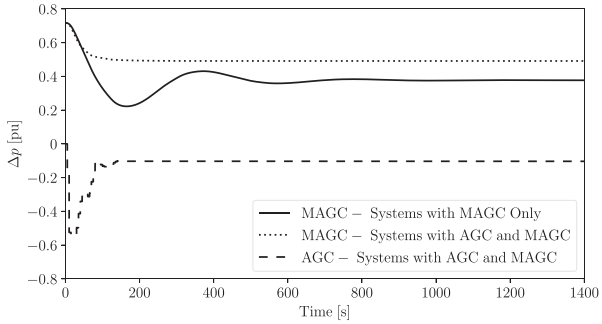

Fig. 16. Secondary frequency controller signals for the scenarios with MAGC only and with both MAGC and AGC.

the controller even less effective, i.e. almost an open loop. The interested reader is referred to [25] for such an example. As for the case of the AGC, the best solution appears to be that of using short dispatch intervals.

3) Systems With AGC and MAGC: This scenario considers a common scenario, i.e. power systems equipped with both an AGC and a real-time electricity market. The AGC considered here has a time interval of 4 s. Simulations are solved considering the same load outage as in the previous section.

The transient response of the system following the contingency is depicted in Fig. 15. The inclusion of the AGC removes the limit cycle. It appears that, if the system includes an AGC, then the discretization of the real-time market does not cause instability issues. It is also interesting to note that using a continuous MAGC leads to a lower frequency nadir. This is due to the dynamic coupling between the dynamics of the MAGC and the AGC. Depending on the severity of the frequency variations, the system operator may have to implement corrective actions, e.g., load shedding. However, a discussion on corrective actions is outside the scope of this paper.

4) Economic Impact of Systems With and Without an AGC: This scenario discusses the differences with respect to the profit of the generating units that are part of systems that include only MAGC controller, and both AGC and MAGC. We assume that both MAGC controllers utilizes a time interval of 60 s, whereas the AGC utilizes a time interval of 4 seconds. Fig. 16 shows the outputs of the controllers for the generator at bus 1, for the scenarios with MAGC only, and with both AGC and MAGC.

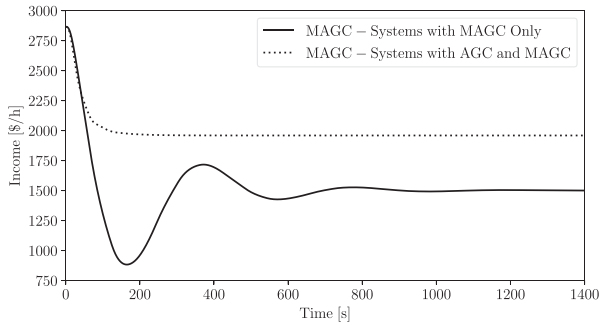

Fig. 17. Profit of generator 1 for the scenarios with MAGC only and with both MAGC and AGC.

It is interesting to see that the MAGC only controller contributes more (by decreasing more its output in response to the contingency) compared to the same controller when the system includes both MAGC and AGC. This is due to the fact that in the scenario that includes both controllers, the AGC is the dominant controller (being faster) and takes care of power mismatches. For this reason, the profit of generating units that participate in the MAGC only is less compared to the profit of the same generating units that are part of power systems with MAGC and AGC (the other way round is true if a generator is lost). This is better shown in Fig. 17 where the income of the first generator is depicted for both scenarios considered in this section.

V. Inclusion of Non-Synchronous Devices

So far we have studied the impact of discrete AGC and MAGC using conventional power systems. However, it is also relevant to study such an impact on power systems with high shares of non-synchronous devices. The impact of wind power penetration is considered. With this aim, the New England IEEE 39-bus system [26] is utilized along with the market data taken from [6]. The contingency is the outage at $t = 1$ s of the load located at bus 3. For simulation purposes a MAGC with a time interval of 120 s (chosen on purpose as it is the worse case scenario) and gain $K_E = 15$ are used. Whereas for the AGC a time interval of 4 s and gain $K_o = 2$ is used. The focus is on the transient response of the center of inertia following the contingency. Three scenarios are considered: (i) base case with conventional generation; (ii) 25% penetration of wind generation; and (iii) 50% penetration of wind generation. For a fair comparison, all scenarios have same loading level, control and network topology.

A. Wind Power Modeling in Real-Time Electricity Markets

Nowadays, in most electricity markets worldwide, wind power producers bid in the same way and follow same rules as conventional power plants. For instance, wind power plants are responsible for power deviations with respect to the values scheduled in day-ahead market. In this context, following the structure of the original dynamic market model in (8)-(9), one can write the equation that models Wind Power Plants (WPPs) behavior with respect to their marginal cost and the price λ, as

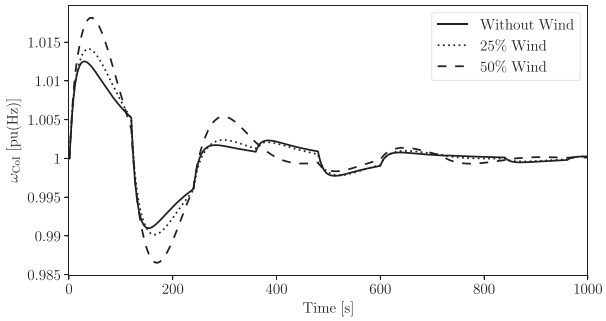

Fig. 18. Transient response of ω_{CoI} for different wind power shares.

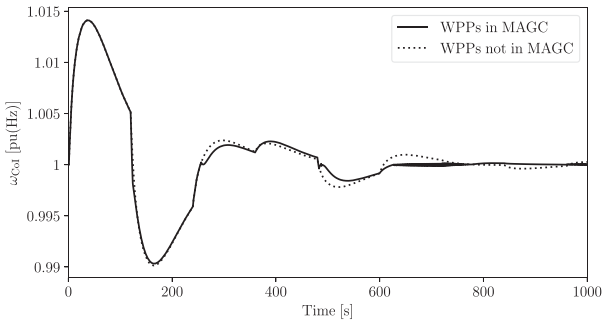

Fig. 19. Transient response of the ω_{CoI} for WPPs included and not included in to the MAGC, respectively.

follows:

$$T_{w,h}\,\dot{p}_{w,h} = \lambda - c_{w,h}\,p_{w,h} - b_{w,h}\,, \quad h = 1, \ldots, n_w\,, \quad (11)$$

where $p_{w,h}$, $T_{w,h}$, $c_{w,h}$, $b_{w,h}$ have same meaning as in (9).

1) Marginal Cost of Wind Power Equal to Zero: In general, the marginal cost of wind is assumed to be zero, i.e.:

$$c_{w,h}p_{w,h} - b_{w,h} = 0\,,$$

and, from (11), we have:

$$T_{w,h}\,\dot{p}_{w,h} = \lambda\,. \quad (12)$$

Equation (12) is a pure integrator. This means that the WPPs will try to dynamically integrate and set the price $\lambda = 0$. As shown earlier in the paper, a pure integrator tends to be unstable. Thus, the WPPs will integrate until their output reaches a maximum power limit. In the same vein, if:

$$c_{w,h}P_{w,h} + b_{w,h} < 0\,,$$

i.e. the WPPs bid negative prices, then from the dynamic point of view their market secondary control is unstable. However, this does not mean that WPPs drives the system to instability, but just that they are going to generate their maximum power all the time.

To simulate this case, we assume that the system includes both AGC and MAGC and show the transient behavior of ω_{CoI} in Fig. 18. The scenarios with non-synchronous devices, i.e., the scenarios with inclusion of wind generation, worsen the performance of both AGC/MAGC controllers, and consequently the dynamic performance of the system. These results indicate that future power systems with high shares of wind power will require much shorter dispatch periods compared to, for example, conventional power systems (see Section IV-D1), in order to avoid possible instabilities.

2) Marginal Cost of Wind Power Different From Zero: If the share of WPPs in the electricity market increases, WPPs may consider acting strategically (i.e., price maker) in order to increase their own profits through intentionally altering the market clearing price. This scenario has been well discussed in the literature, e.g. in reference [27]. In order to become a price maker, WPPs will have to be sufficiently big (otherwise they will be limited), and with a marginal cost that is in the same range as that of other conventional generators. In this scenario, WPPs will participate in the real-time electricity market according to (11), i.e. will be part of the MAGC shown in Fig. 11.

Note that, if they are not coupled with energy storage systems or include some mechanism to provide power reserve, the WPPs can only provide down regulating service, that is, will only decrease their power production. To simulate this scenario, we consider a 25% wind power penetration, i.e. replace 3 conventional generators with WPPs. Furthermore, we assume that the WPPs have the same bids and market data as the conventional power plants. The Spanish electricity market is a real-world example where RESs and conventional power plants bid together [28]. We also assume that the systems includes both AGC and MAGC.

Fig. 19 shows the results for this scenario. It appears that the participation of WPPs in real-time electricity markets does not make a huge difference with respect to the transient response of the system. This is due to the fact that the AGC is the dominant secondary controller, as it is faster than the MAGC and thus contributes more after the occurrence of the contingency (see Fig. 16). We can conclude that, in this scenario, the participation of WPPs in real-time electricity markets does not make a significant contribution to long-term power system dynamics.

VI. Concluding Remarks

This paper studies the impact of discrete secondary frequency controllers on power system stability. The paper considers two secondary frequency controllers, namely, AGC and MAGC. The former is a controller installed in most of the control centers of TSOs, while the latter is a model that reproduces the behavior of real-time electricity markets with short dispatch periods. The findings of the paper are summarized below.

1) AGC: The illustrative example on the impact of discrete AGC on power system stability suggests that increasing too much the execution cycles of the AGC leads to a limit cycle or bang-bang phenomena. The example also shows that increasing the execution cycles of the AGC is comparable to increasing its control gain. Moreover, it is shown that the only effective solution to remove this issue is to keep as short as possible the AGC execution cycles. This is not a major constraint as, in practice, the AGC installed in the control centers of TSOs uses execution cycles that vary in the range of 2 to 6 s, which do not create instability issues.

2) MAGC: The formal analogy between the AGC and real-time electricity markets and the results of the illustrative example indicate that if future real-time electricity markets will be based on the power imbalance in order to update the electricity price and use dispatch periods that range from some tens of seconds up to few minutes then these markets might lead to some sort of limit-cycles and/or power system instability. There are two relevant scenarios, as follows.

- Power systems that do not have installed an AGC and/or have some sort of not-perfect-tracking AGC. In these systems, the real-time electricity markets should use very short dispatch periods, i.e. similar to the ones utilized with the AGC, or should not be based on the power imbalance (open-loop electricity market).
- Power systems with an AGC. In this case, real-time electricity markets can be based on power imbalance as a criterion to update the electricity price and use long dispatch periods. In this scenario, however, the profit of generators that participate in systems with MAGC vary considerably depending on the disturbance and the dynamic of the conventional AGC.

3) Impact of Wind Power Penetration: Section V shows that integrating more wind power generation into power systems worsen the performance of both AGC controllers, and consequently the power system dynamic performance. Simulation results show that power systems that are based on real-time electricity markets should use shorter dispatch periods compared to the case without wind power. Regarding the differences with respect to the participation of WPPs in real-time electricity markets, the case study shows that this participation does not necessarily mean an improvement in the dynamic performance of the system.

Finally, future works will focus on the impact of other relevant discrete secondary controllers of power systems, e.g., the secondary voltage control and hierarchical controllers of microgrids.

REFERENCES

[1] H. Bevrani, *Robust Power System Frequency Control*. NewYork, NY, USA: Springer, 2009.

[2] F. Milano, F. Dörfler, G. Hug, D. J. Hill, and G. Verbič, "Foundations and challenges of low-inertia systems (invited paper)," in *Proc. Power Syst. Comput. Conf.*, Jun. 2018, pp. 1–25.

[3] D. Apostolopoulou, P. W. Sauer, and A. D. Domínguez-Garcia, "Automatic generation control and its implementation in real time," in *Proc. 47th Hawaii Int. Conf. Syst. Sci.*, 2014, pp. 2444–2452.

[4] V. Pandurangan, H. Zareipour, and O. Malik, "Frequency regulation services: A comparative study of select north american and european reserve markets," in *Proc. North Amer. Power Symp.*, 2012, pp. 1–8.

[5] Aemo, "Aemo annual report 2018-leading the transformation." [Online]. Available: https://www.aemo.com.au/-/media/files/about_aemo/annual-report/aemo-annual-report-2018.pdf

[6] F. L. Alvarado, J. Meng, C. L. DeMarco, and W. S. Mota, "Stability analysis of interconnected power systems coupled with market dynamics," *IEEE Trans. Power Syst.*, vol. 16, no. 4, pp. 695–701, Nov. 2001.

[7] C. Zhang, L. Jiang, Q. H. Wu, Y. He and M. Wu, "Further results on delay-dependent stability of multi-area load frequency control," *IEEE Trans. Power Syst.*, vol. 28, no. 4, pp. 4465–4474, Nov. 2013.

[8] L. Xu, Q. Guo, Z. Wang and H. Sun, "Modeling of time-delayed distributed cyber-physical power systems for small-signal stability analysis," *IEEE Trans. Smart Grid*, vol. 12, no. 4, pp. 3425–3437, Jul. 2021.

[9] X. Shangguan *et al.*, "Robust load frequency control for power system considering transmission delay and sampling period," *IEEE Trans. Ind. Inform.*, vol. 17, no. 8, pp. 5292–5303, Aug. 2021.

[10] R. Venkateswaran and Y. H. Joo, "Retarded sampled-data control design for interconnected power system with DFIG-based wind farm: LMI approach," *IEEE Trans. Cybern.*, to be published, doi: 10.1109/TCYB.2020.3042543.

[11] E. Fridman, "A refined input delay approach to sampled-data control," *Automatica*, vol. 46, no. 2, pp. 421–427, 2010.

[12] H. Gao, S. Xue, S. Yin, J. Qiu, and C. Wang, "Output feedback control of multirate sampled-data systems with frequency specifications," *IEEE Trans. Control Syst. Technol.*, vol. 25, no. 5, pp. 1599–1608, Sep. 2017.

[13] T. Stegink, C. De Persis, and A. van derSchaft, "A unifying energy-based approach to stability of power grids with market dynamics," *IEEE Trans. Autom. Control*, vol. 62, no. 6, pp. 2612–2622, Jun. 2017.

[14] P. Ferraro, E. Crisostomi, M. Raugi, and F. Milano, "Analysis of the impact of microgrid penetration on power system dynamics," *IEEE Trans. Power Syst.*, vol. 32, no. 5, pp. 4101–4109, Sep. 2017.

[15] J. Nutaro and V. Protopopescu, "The impact of market clearing time and price signal delay on the stability of electric power markets," *IEEE Trans. Power Syst.*, vol. 24, no. 3, pp. 1337–1345, Aug. 2009.

[16] W. Chiu, H. Sun, and H. V. Poor, "Energy imbalance management using a robust pricing scheme," *IEEE Trans. Smart Grid*, vol. 4, no. 2, pp. 896–904, Jun. 2013.

[17] F. Milano, *Power System Modelling and Scripting*. London, U.K.: Springer, 2010.

[18] Y. G. Rebours, D. S. Kirschen, M. Trotignon, and S. Rossignol, "A survey of frequency and voltage control ancillary services-part I: Technical features," *IEEE Trans. Power Syst.*, vol. 22, no. 1, pp. 350–357, Feb. 2007.

[19] V. Pavlovsky and A. Steliuk, "Modeling of automatic generation control in power systems," in *Power Factory Application Power System Analysis*, Springer, 2014, pp. 157–173.

[20] Illinois Center for a Smarter Electric Grid (ICSEG), "WSCC 9-Bus System," [Online]. Available: http://publish.illinois.edu/smartergrid/wscc-9-bus-system/

[21] F. Milano, "A python-based software tool for power system analysis," in *Proc. IEEE PES General Meeting*, Vancouver, BC, Jul. 2013, pp. 1–5.

[22] F. L. Alvarado *et al.*, "The dynamics of power system markets," University of Wisconsin-Madison, PSERC Research Report, pp. 97–01, 1997.

[23] =plus 4minus , "Trading on epex spot 2019-2020." [Online]. Available: http://static.epexspot.com/document/41159/19-10-23_Trading%20Brochure.pdf

[24] EirGrid & SONI, "Balancing market principles statement. A guide to scheduling and dispatch in the single electricity market," 2020.

[25] T. Kërçi, J. Giraldo, and F. Milano, "Analysis of the impact of sub-hourly unit commitment on power system dynamics," *Int. J. Elect. Power Energy Syst.*, vol. 119, 2020, Art. no. 105819.

[26] Illinois Center for a Smarter Electric Grid (ICSEG), "IEEE 39-Bus System," [Online].Available: http://publish.illinois.edu/smartergrid/ieee-39-bus-system/

[27] S. Delikaraoglou, A. Papakonstantinou, C. Ordoudis, and P. Pinson, "Price-maker wind power producer participating in a joint day-ahead and real-time market," in *Proc. 12th Int. Conf. Eur. Energy Market*, 2015, pp. 1–5.

[28] J. Barquín, "The new spanish electricity market design," in *Proc. 9th Conf. Energy Econ. Technol.*, Dresden, Germany, 2014, pp. 1–10.

Taulant Kërçi (Student Member, IEEE) received the B.Sc. and M.Sc. degrees in electrical engineering from the Polytechnic University of Tirana, Tirana, Albania, in 2011 and 2013, respectively. Since February 2018, he has been working toward the Ph.D. degree with University College Dublin, Dublin, Ireland. From June 2013 to October 2013, he was with Metering and New Connection Department, Albanian DSO. From November 2013 to January 2018, he was with TSO, SCADA/EMS office. His research interests include power system dynamics and co-simulation of power systems and electricity markets.

Mohammed Ahsan Adib Murad received the B.Sc. degree in electrical engineering from the Islamic University of Technology, Gazipur, Bangladesh, in 2009 and double M.Sc. degrees in smart electrical networks and systems from KU Leuven, Leuven, Belgium, and the KTH Royal Institute of Technology, Stockholm, Sweden, in 2015. He is currently working toward the Ph.D. degree with the School of Electrical and Electronic Engineering, University College Dublin, Dublin, Ireland. He is currently an Application Engineer with DIgSILENT GmbH, Germany. His research interests include dynamic modeling and stability analysis of power systems.

Ioannis Dassios received the Ph.D. degree in applied mathematics from the Department of Mathematics, University of Athens, Athens, Greece, in 2013. He was a Postdoctoral Researcher and a Teaching Fellow in optimization with the School of Mathematics, University of Edinburgh, Edinburgh, U.K. He was also a Research Associate with Modelling and Simulation Centre, University of Manchester, Manchester, U.K., and as a Research Fellow with MACSI, University of Limerick, Limerick, Ireland. He is currently a UCD Research Fellow with University College Dublin, Dublin, Ireland.

Federico Milano (Fellow, IEEE) received the M.E. and Ph.D. degrees in electrical engineering from the University of Genoa, Genoa, Italy, in 1999 and 2003, respectively. From 2001 to 2002, he was with the University of Waterloo, Waterloo, ON, Canada. From 2003 to 2013, he was with the University of Castilla-La Mancha, Ciudad Real, Spain. In 2013, he joined University College Dublin, Dublin, Ireland, where he is currently a Professor of power systems control and protections. His research focuses on power systems modeling, control, and stability analysis.